

Magnetic properties of [NiFe/Au/Co/Au] multilayers

magnetostatic coupling and giant magnetoresistance

Zmniejszona jakość ilustracji
Low quality version
Zakopane 2009

Maciej Urbanik, Feliks Stobiecki, Bogdan Szymański
Institute of Molecular Physics, Polish Academy of Sciences

Magnetic properties of [NiFe/Au/Co/Au] multilayers

magnetostatic coupling and giant magnetoresistance

Cooperation between:

Institute of Molecular Physics, Polish Academy of Sciences, Poznań, Poland

Prof. A. Ehresmann
Department of Physics, University of Kassel, Kassel, Germany

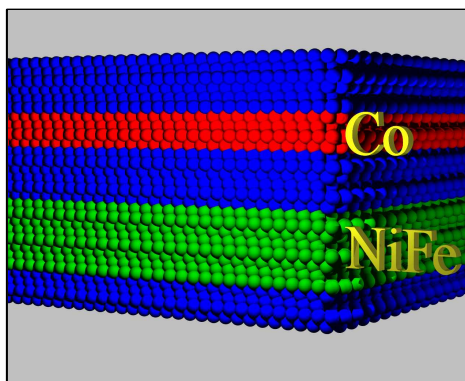
Prof. M. Kopcewicz
Institute of Electronic Materials Technology, Warszawa, Poland

Prof. A. Maziewski
Laboratory of Magnetism, Faculty of Physics, University of Białystok, Poland

Magnetic properties of [NiFe/Au/Co/Au] multilayers

- Introduction
- Magnetic properties
- Giant magnetoresistance
- Magnetostatic coupling
- Magnetic patterning
- Conclusions

Introduction



Substrate:
naturally oxidized
Si(100)

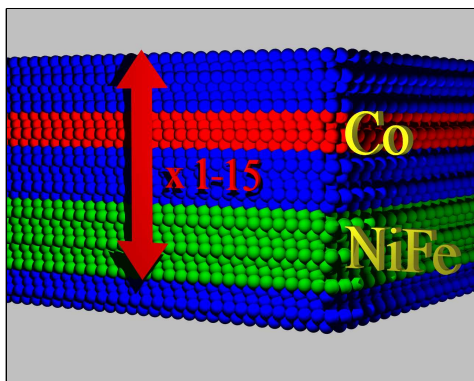
$t_{\text{Co}(\text{CoFe})} = 0.2-1.5 \text{ nm}$

$t_{\text{NiFe}} = 0.5-4 \text{ nm}$

$t_{\text{Au}} = 1.5-3 \text{ nm}$

Magnetron sputtering

Introduction



Substrate:
naturally oxidized
Si(100)

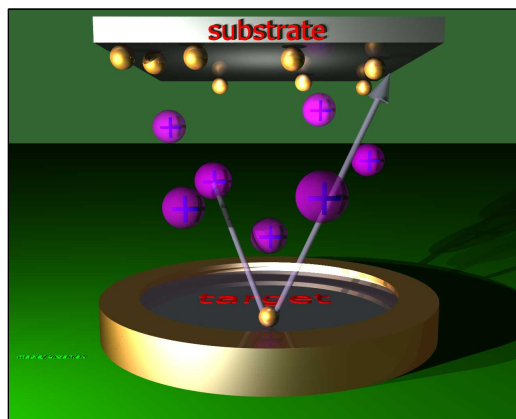
$t_{\text{Co}(\text{CoFe})} = 0.2-1.5 \text{ nm}$

$t_{\text{NiFe}} = 0.5-4 \text{ nm}$

$t_{\text{Au}} = 1.5-3 \text{ nm}$

Magnetron sputtering

Introduction



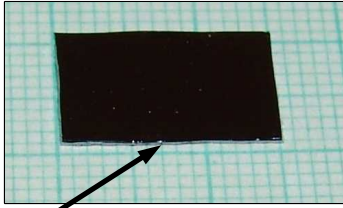
Target:
NiFe, Au, Co

Substrate:
Si(100), glass,
adhesive tape

Magnetron sputtering

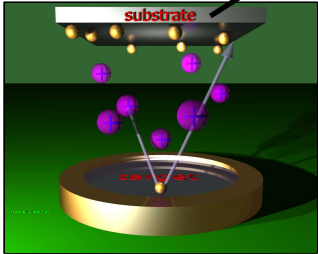
Target-
negative potential

Introduction



Target:
NiFe, Au, Co

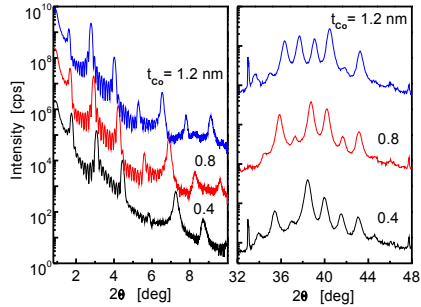
Substrate:
Si(100), glass,
adhesive tape



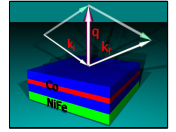
Magnetron sputtering

Target-negative potential

Introduction



Crystalline structure

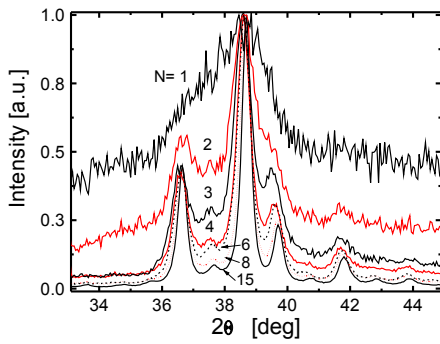


good periodicity
defined fcc(111) texture

[Ni₈₀Fe₂₀(2 nm)/Au(1.9 nm)/Co(t_{Co})/Au(1.9 nm)]₁₀
Cu Kα 0.154nm

Introduction

Crystalline structure

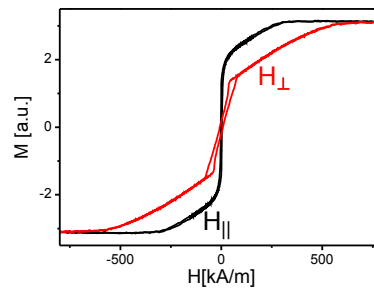


"the profile for MLs with N = 3 shows all features typical of profiles for large N."

[Ni₈₀Fe₂₀(2 nm)/Au(3 nm)/Co(0.8)/Au(3 nm)]_N
Cu Kα 0.154nm

B. Szymański et al., Acta. Phys. Polon. 113, 205 (2008)

Magnetic properties



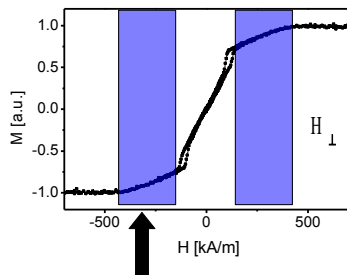
NiFe – magnetic easy axis in-plane

Co – magnetic easy axis perpendicular to plane of the sample

- Small field range of hysteresis with field applied perpendicularly is characteristic of systems with **stripe domains**.
- In both field configurations NiFe and Co layers reverse quasi independently.

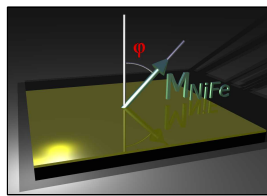
[Ni₈₀Fe₂₀(2 nm)/Au(1.9 nm)/Co(0.8 nm)/Au(1.9 nm)]₁₀

Magnetic properties



Reversal of NiFe only

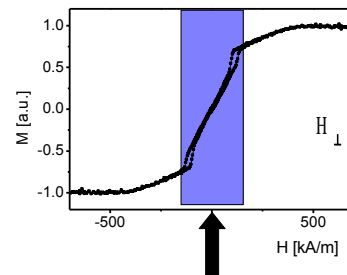
$$K_u = \frac{1}{2} \mu_0 (M_S^{NiFe})^2$$



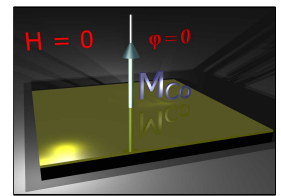
Shape anisotropy:

$$\cos(\varphi) = \frac{H}{M_S}$$

Magnetic properties

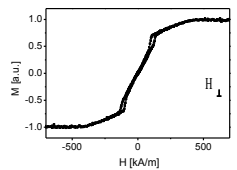
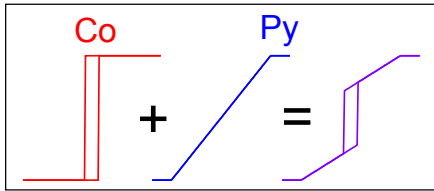


Simultaneous reversal of NiFe and Co



An easy axis of the Co layers is perpendicular to surface of multilayer.

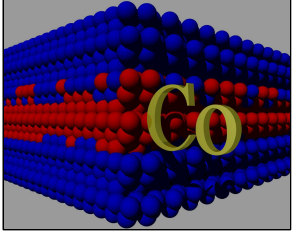
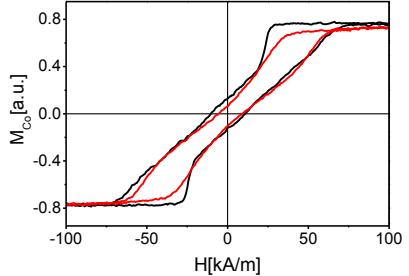
Magnetic properties



In the first approximation Co and NiFe layers can be thought of as uncoupled.

$M(H)$ dependence of the NiFe/Au/Co structure is then an arithmetic sum of the $M(H)$ dependencies of Co and NiFe layers.

Magnetic properties

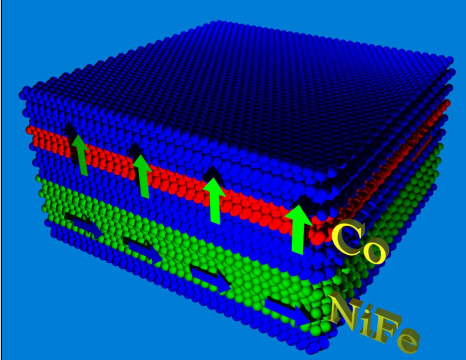


$[\text{Ni}_{80}\text{Fe}_{20}(2 \text{ nm})/\text{Au}(1.9 \text{ nm})/\text{Co}(0.6 \text{ nm})/\text{Au}(1.9 \text{ nm})]_{10}$
 $[\text{Co}(0.6 \text{ nm})/\text{Au}(4.4 \text{ nm})]_{15}$

NiFe sublayers do not considerably influence the reversal of Co sublayers.

Magnetic properties

Stripe domains



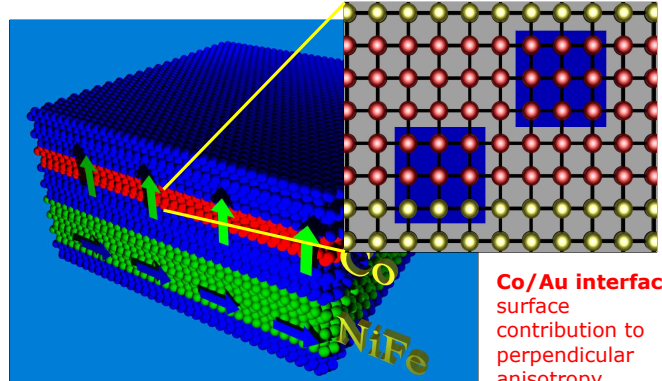
K_{eff} strongly depends on t_{Co}

Co sublayers: perpendicular effective magnetic anisotropy for $t_{\text{Co}} = 0.5 \div 1.2 \text{ nm}$

$$K_{\text{eff}} = \frac{2K_{1s}}{t_{\text{Co}}} + K_{1v} - \frac{1}{2}\mu_0(M_S^{\text{Co}})^2$$

Magnetic properties

Stripe domains

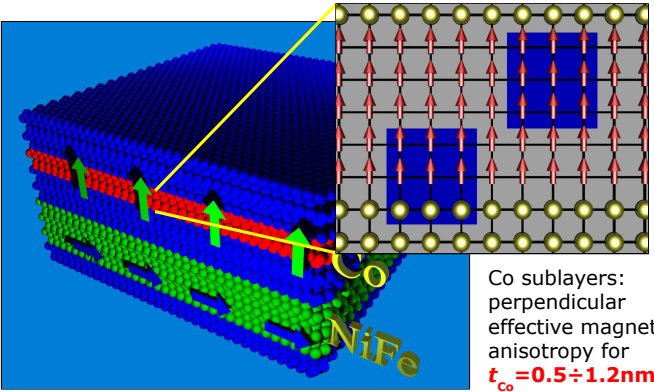


Co/Au interface-surface contribution to perpendicular anisotropy

$$K_{\text{eff}} = \frac{2K_{1s}}{t_{\text{Co}}} + K_{1v} - \frac{1}{2}\mu_0(M_S^{\text{Co}})^2$$

Magnetic properties

Stripe domains

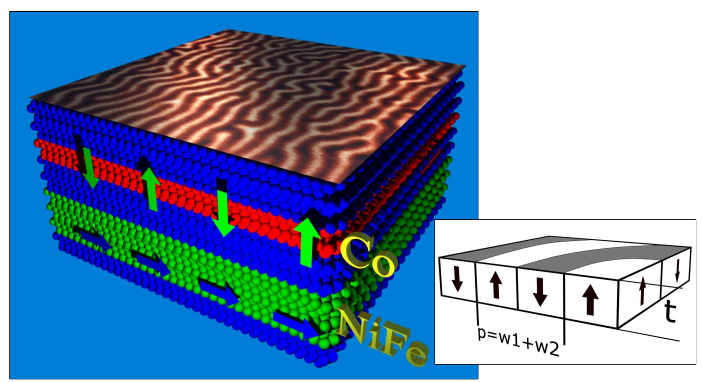


Co sublayers: perpendicular effective magnetic anisotropy for $t_{\text{Co}} = 0.5 \div 1.2 \text{ nm}$

$$K_{\text{eff}} = \frac{2K_{1s}}{t_{\text{Co}}} + K_{1v} - \frac{1}{2}\mu_0(M_S^{\text{Co}})^2$$

Magnetic properties

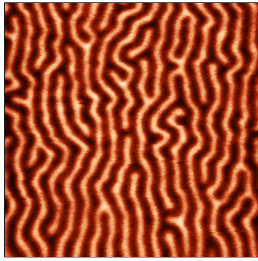
Stripe domains



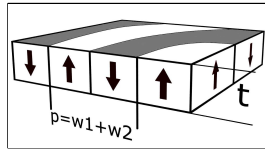
Magnetic Force Microscopy confirms the presence of the stripe domain structure characteristic for systems with perpendicular anisotropy.

Magnetic properties

Stripe domains

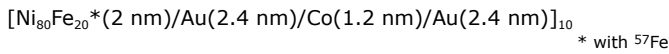


AC demagnetization
5x5μm²



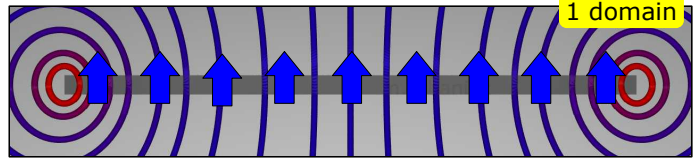
spatial period 400-1000 nm

Spatial period of the stripe domain structure depends strongly on the thicknesses of Co and Au sublayers.



Magnetic properties

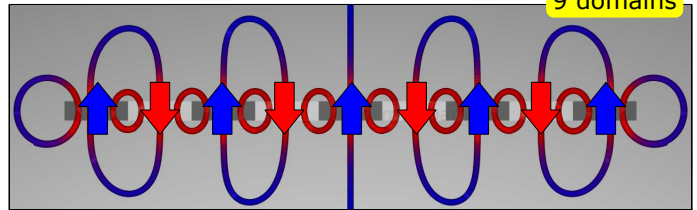
Stripe domains



1 domain

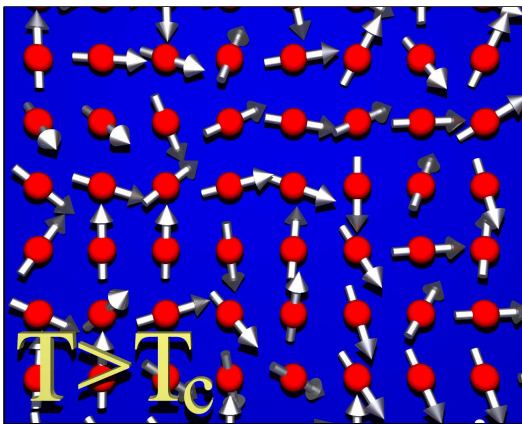
Division into **the magnetic stripe domains** increases the magnetic induction within the layer and leads to the decrease of magnetostatic energy:

$$E_{magn} = -\vec{B} \cdot \vec{M}$$



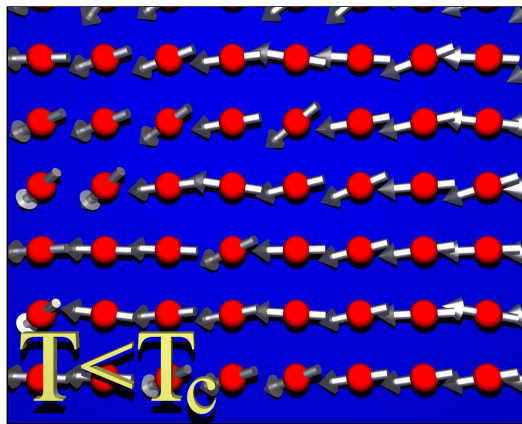
9 domains

Giant magnetoresistance



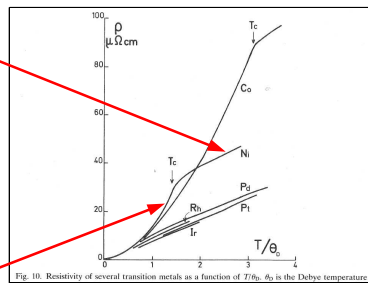
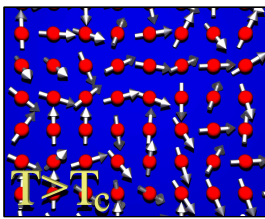
T_{Curie}:
Fe 1044 K
Co 1388 K
Ni 627 K
NiFe 660 K

Giant magnetoresistance



T_{Curie}:
Fe 1044 K
Co 1388 K
Ni 627 K
NiFe 660 K

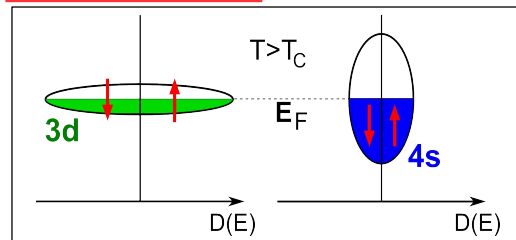
Giant magnetoresistance



Below Curie temperature the resistance of ferromagnetic materials decreases below that of non-ferromagnetic metals.

I.A.Campbell, A.Fert, in "Ferromagnetic Materials" 1982

Giant magnetoresistance

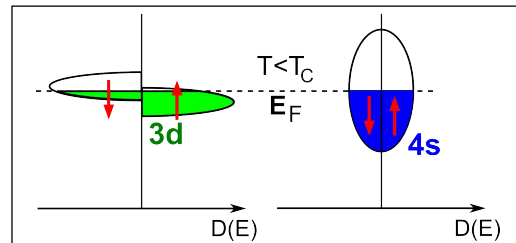


Scattering:

$s\uparrow \rightarrow d\uparrow$

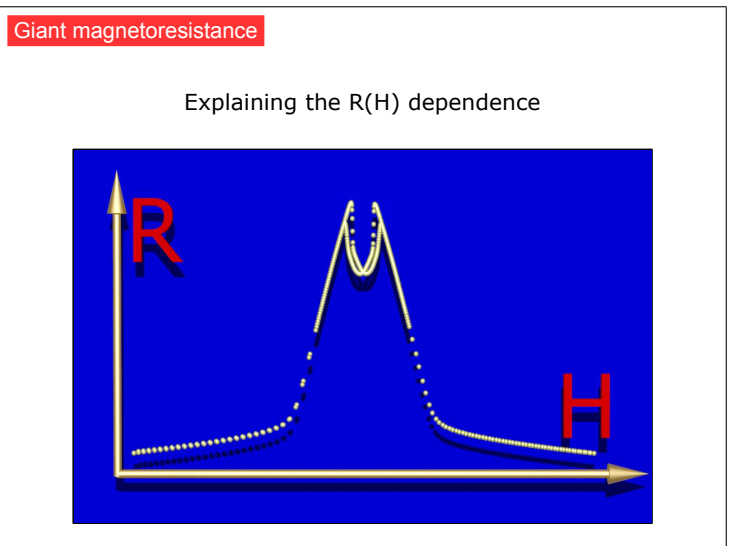
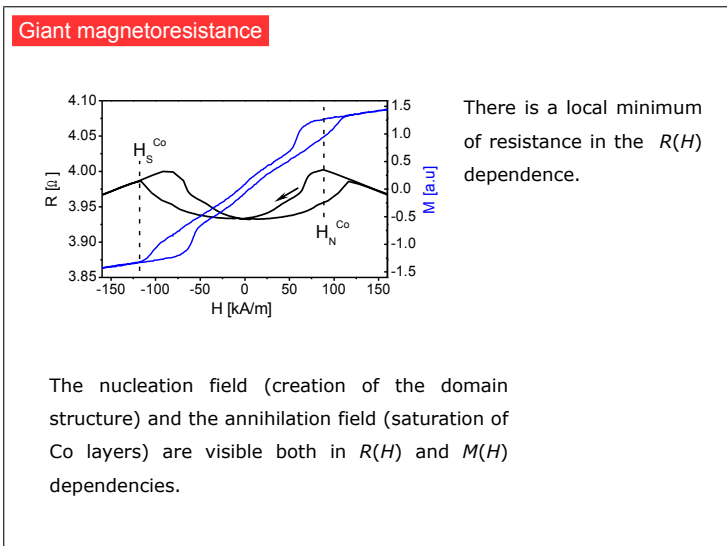
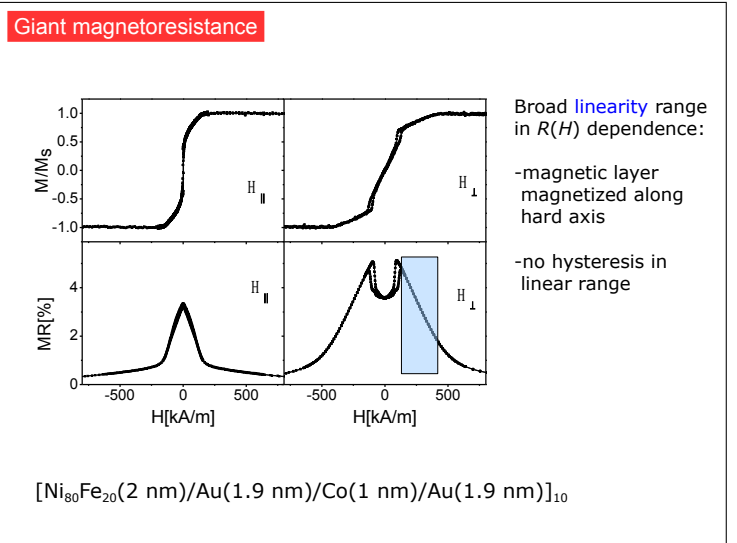
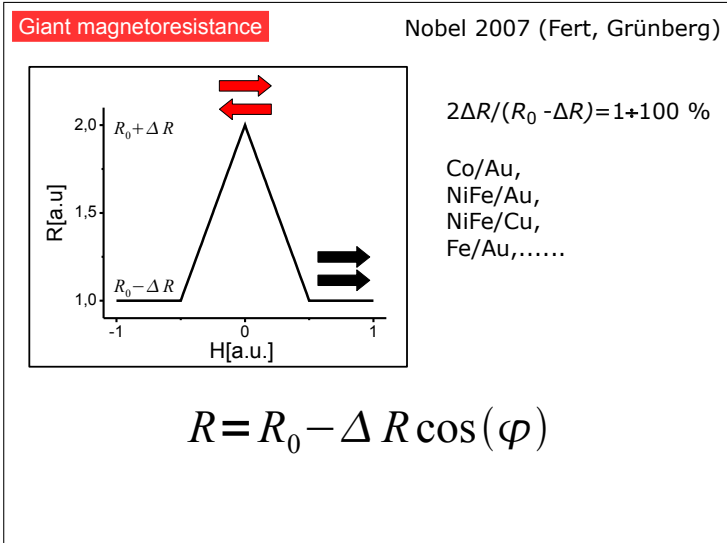
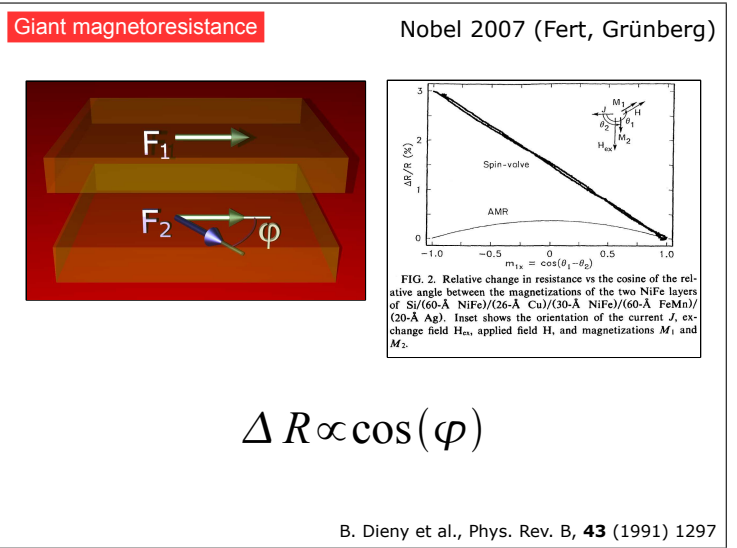
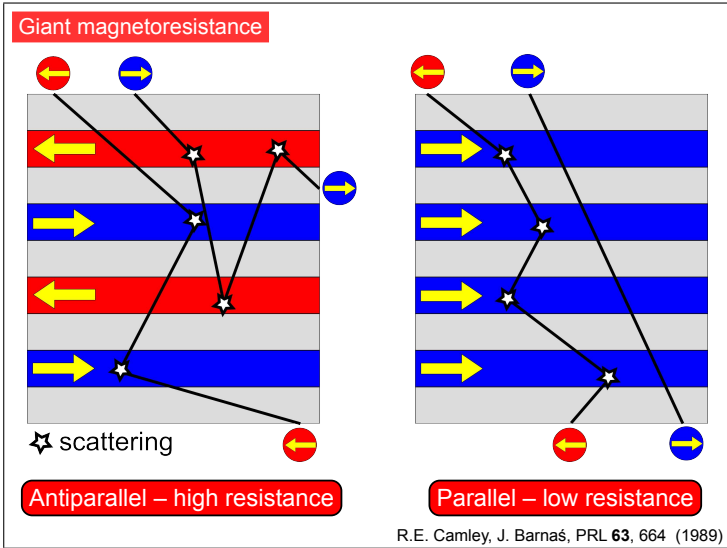
$s\downarrow \rightarrow d\downarrow$

$\rho \sim D(E_F)$



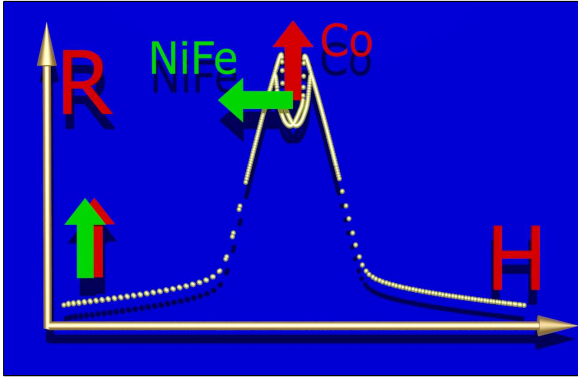
$s\uparrow \rightarrow d\uparrow$

$s\downarrow \rightarrow d\downarrow$



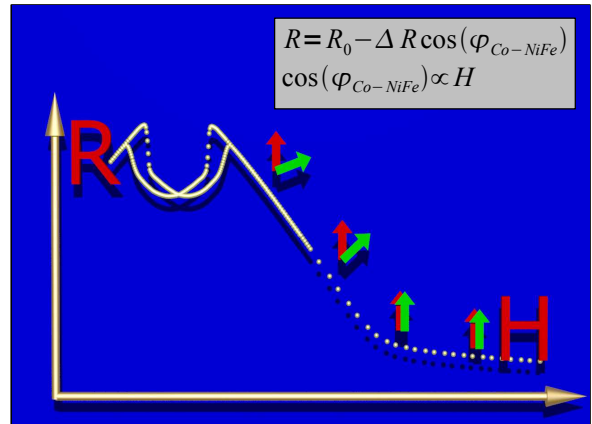
Giant magnetoresistance

Explaining the R(H) dependence



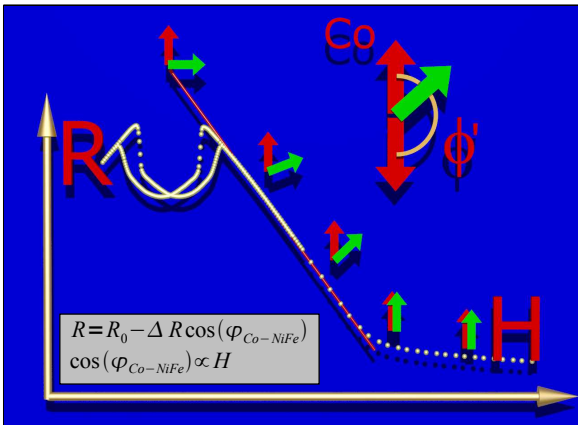
Giant magnetoresistance

Explaining the R(H) dependence



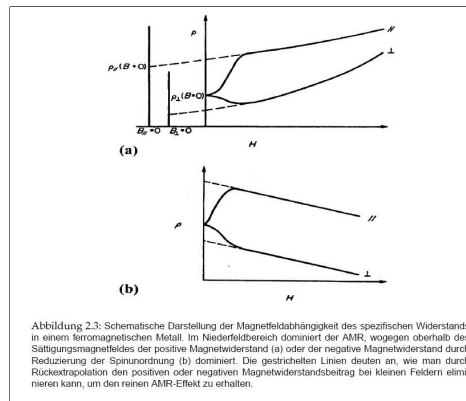
Giant magnetoresistance

Explaining the R(H) dependence



Giant magnetoresistance

Anisotropic magnetoresistance



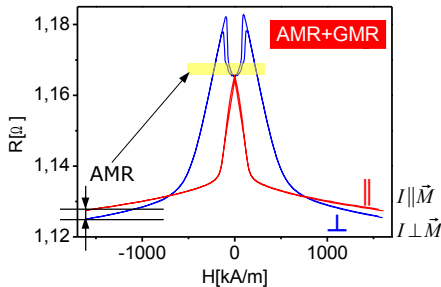
AMR in NiFe alloys reaches 5%.

resistance of the system depends on the angle between the measuring current and the local magnetic moment

Grundlagen der Magnetelektronik, Rudolf Gross, Achim Marx, Garching, Oktober 2000
<http://www.wmi.badw-muenchen.de/teaching/LectureNotes/>

Giant magnetoresistance

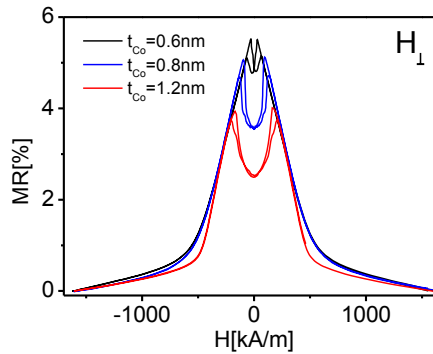
Anisotropic magnetoresistance



Anisotropic magnetoresistance is too small to account for the observed local minima of resistance.

$[Ni_{80}Fe_{20}(2\text{ nm})/Au(1.9\text{ nm})/Co(1\text{ nm})/Au(1.9\text{ nm})]_{10}$

Giant magnetoresistance



A relative "depth" of resistance minimum is a strong function of Co layers thickness.

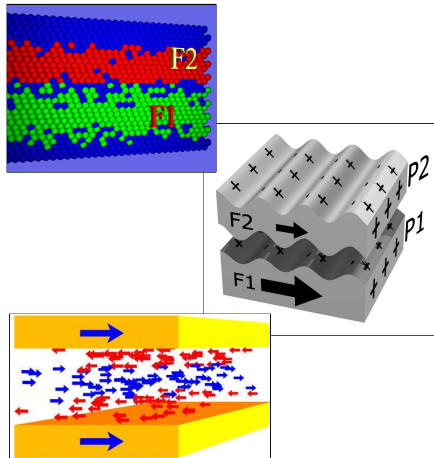
?

Magnetostatic coupling

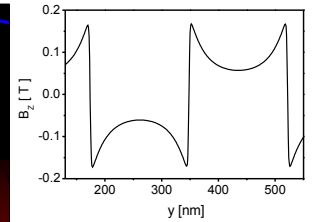
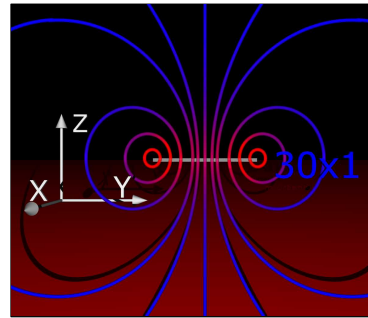
$[Ni_{80}Fe_{20}(2\text{ nm})/Au(1.9\text{ nm})/Co(t_{Co})/Au(1.9\text{ nm})]_{10}$

Interlayer coupling in magnetic multilayers

- coupling through magnetic bridging
- magnetostatic coupling
- Ruderman-Kittel-Kasuya-Yosida like coupling



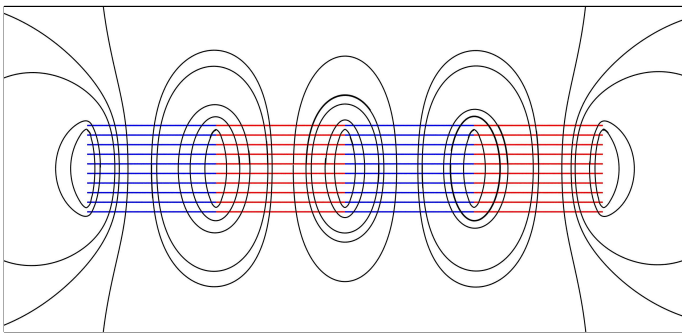
Magnetostatic coupling



Model:
Domains width: 174 nm
 $t_{Co}=0.6$ nm **10 Co layers**

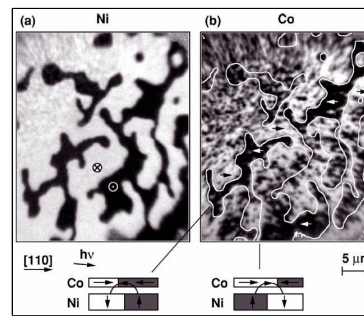
Magnetic fields that originate from the stripe domain structure in $[\text{NiFe}/\text{Au}/\text{Co}/\text{Au}]_n$ multilayers are of the order of 0.1 T.

Magnetostatic coupling

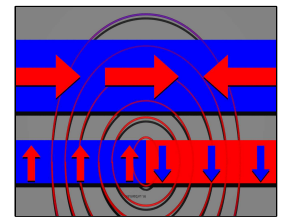


Magnetic field of the stack of the infinite "stripe domains" (from Biot-Savart law). Domain width=100, thickness=1, multilayer period=7.

Magnetostatic coupling



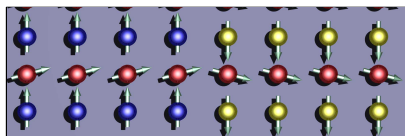
photoemission electron microscopy (PEEM) + X ray magnetic circular dichroism (XMCD)



-Cu(001)/Ni/Cu/Co
-Cu - wedge (1ML/10m)
-electron beam evaporation
-Ni - perpendicular anisotropy
-field of Ni DW in Co: 2500e

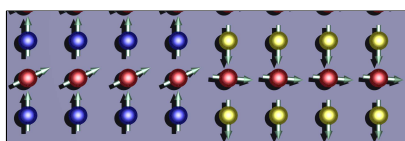
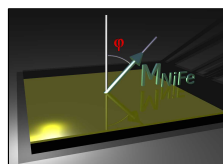
W. Kuch, L. I. Chelaru, K. Fukumoko, F. Porrati, F. Offi, M. Kotsugi, J. Kirchner, Phys. Rev. B **67**, 214403 (2003)

Magnetostatic coupling



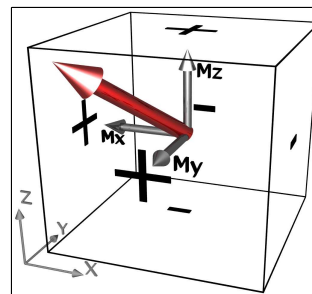
Co $H=H_{\text{domains}}$
NiFe
Co

$$\cos(\varphi_1) = \frac{H_{\text{appl}} + H_d}{M_S^{\text{Co}}} \quad \cos(\varphi_1) = \frac{H_{\text{appl}} - H_d}{M_S^{\text{Co}}}$$



$H=H_{\text{domains}}+H_{\text{appl}}$
 H_{appl}

Magnetostatic coupling



С. В. Вонсовский, МАГНЕТИЗМ «Наука», 1971

Micromagnetic simulation

$$r = [(x_n - x_q)^2 + (z_n - z_q)^2 + (z_n - z_q)^2]^{1/2}$$

$$\phi_m^{(i)} = \frac{1}{4\pi} \frac{(\vec{r} \cdot \vec{r})}{r^3}$$

$$\vec{H} = -\vec{\nabla} \phi$$

$$\phi_m = \frac{1}{4\pi} \int d\tau (\vec{M} \cdot \nabla_q r^{-1})$$

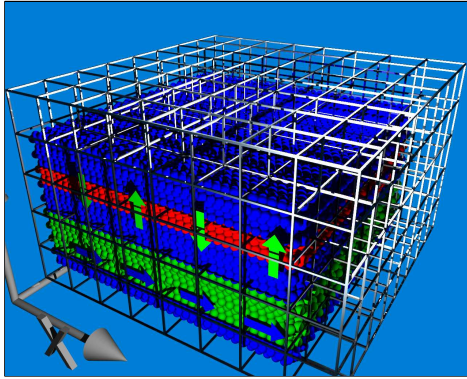
$$(\vec{M} \cdot \nabla_q r^{-1}) = \nabla_q (r^{-1} \vec{M}) - \frac{1}{r} \nabla_q \vec{M}$$

$$\phi_m = \frac{1}{4\pi} (-\int d\tau \frac{\nabla_q \vec{M}}{r} + \oint dS \frac{\vec{n} \cdot \vec{M}}{r})$$

"Magnetic charges" present within the volume of the magnetized body And on its outer boundaries are the sources of magnetic field.

Magnetostatic coupling

Micromagnetic simulation

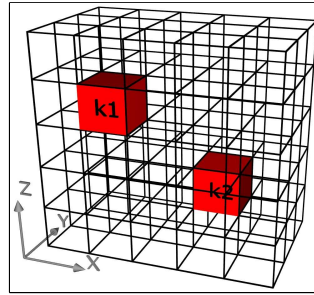


A single cell contains MANY atoms.

Continuous approximation - the magnetization is a continuous function of the position.

Magnetostatic coupling

Micromagnetic simulation



LLG equation: $\dot{\vec{m}} = \frac{\vec{M}}{M_s}$

$$\frac{d\vec{m}}{dt} = \gamma_0(\vec{m} \times \vec{H}_{eff}) + \alpha[\vec{m} \times \frac{d\vec{m}}{dt}]$$

$$\vec{H}_{eff} = \frac{-1}{\mu_0 M_s} \frac{\delta \epsilon}{\delta \vec{m}}$$

$$\vec{H}_{eff} = \frac{A}{\mu_0 M_s} \frac{\delta(\nabla \vec{m})^2}{\delta \vec{m}} - \frac{1}{\mu_0 M_s} \frac{\delta \epsilon_K}{\delta \vec{m}} + \vec{H}_{appl} + \vec{H}_d$$

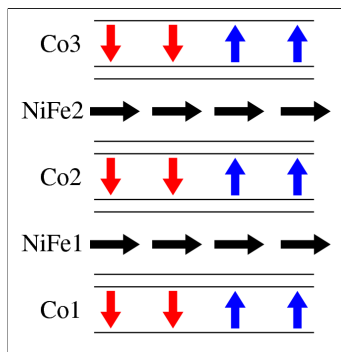
\vec{H}_{eff} = "exchange energy" + "anisotropy energy" + "external field" + "own field"

Magnetostatic interactions between cells have of a **long-range character**.

J. E. Milat, M. J. Donahue
Handbook of Magnetism and Advanced Magnetic Materials, John Wiley & Sons 2007

Magnetostatic coupling

Micromagnetic simulation*

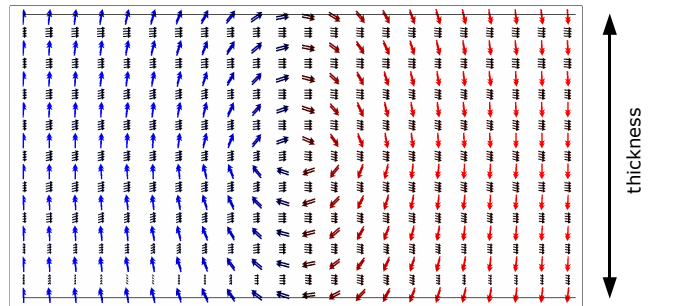


- simulation of remanent state
- starting configuration-stripe domains in Co sublayers
- starting configuration-monodomain state in NiFe sublayers

*Simulation with free oommf package from NIST; $(1 \times 1 \mu\text{m}^2) \times 55\text{nm}$; Co domains 200 nm wide; $\alpha=0.5$; regular mesh with cell size of $(5 \times 0.5 \times 50 \text{nm}^3)$; stiffness: Co: 30e-12 J/m, NiFe: 13e-12 J/m

Magnetostatic coupling

Micromagnetic simulation*

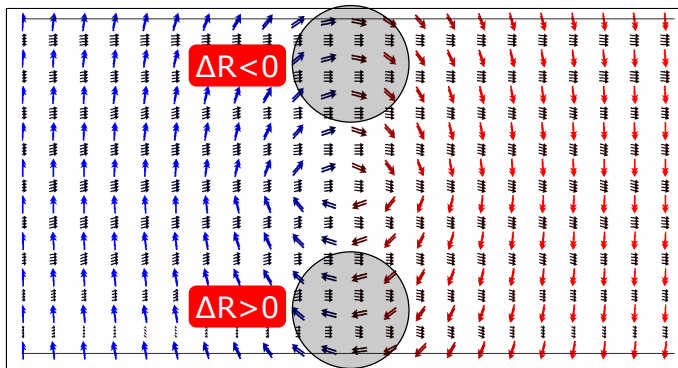


$[\text{Co}(1\text{nm})/\text{Au}(1.5\text{nm})/\text{Ni}_{90}\text{Fe}_{10}(2\text{ nm})/\text{Au}(1.5\text{ nm})]_5/\text{Co}(1\text{nm})$ $H=0$

*Simulation with free oommf package from NIST; $(1 \times 1 \mu\text{m}^2) \times 55\text{nm}$; Co domains 200 nm wide; $\alpha=0.5$; regular mesh with cell size of $(5 \times 0.5 \times 50 \text{nm}^3)$; stiffness: Co: 30e-12 J/m, NiFe: 13e-12 J/m

Magnetostatic coupling

Micromagnetic simulation

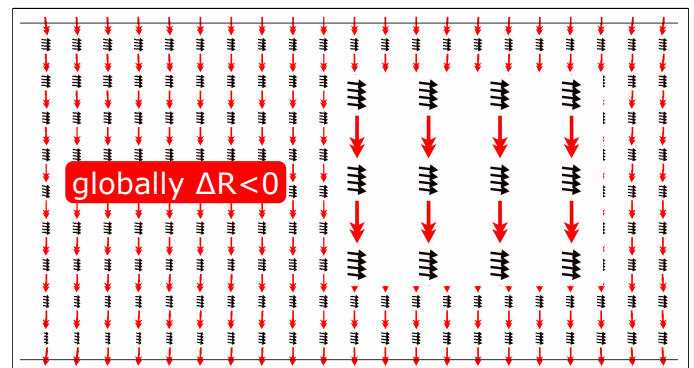


$\Delta R \propto \cos(\varphi)$

$H=0$

Magnetostatic coupling

Micromagnetic simulation

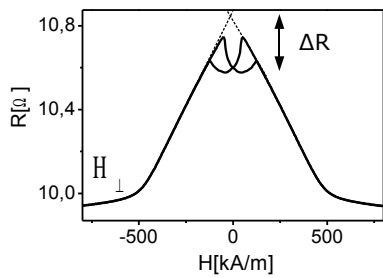


$\Delta R \propto \cos(\varphi)$

$H=0$

Magnetostatic coupling

Micromagnetic simulation

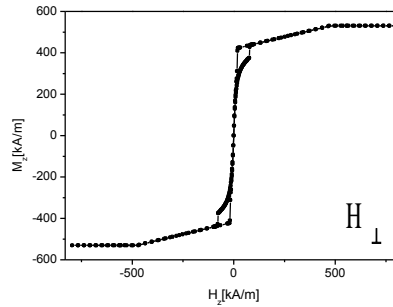


$$\Delta \cos(\phi) = 0.265$$

Magnetostatic interactions between Co and NiFe layers lead to the decrease of the average cosine of the angle between magnetic moments of neighboring sublayers \Rightarrow resistance decrease.

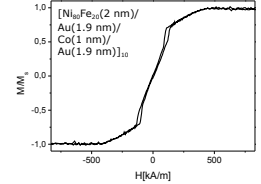
Magnetostatic coupling

Micromagnetic simulation*



Co-perpendicular anisotropy
NiFe-shape anisotropy

measurement:

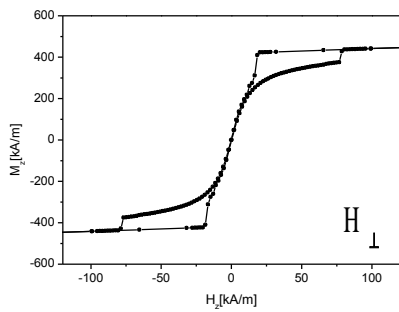


[Co(1nm)/spacer(1nm)/NiFe(1nm)/spacer(1nm)]₄/Co(1nm)

*Simulation with free oommf package from NIST (M.J. Donahue and D.G. Porter); $\alpha=0.5$; regular mesh with cell size of $(5 \times 2000 \times 1 \text{ nm}^3)$; stiffness: Co: $30 \text{e-}12 \text{ J/m}$, NiFe: $13 \text{e-}12 \text{ J/m}$

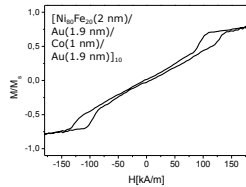
Magnetostatic coupling

Micromagnetic simulation



Co-perpendicular anisotropy
NiFe-shape anisotropy

measurement:

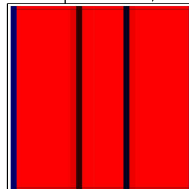
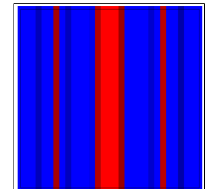
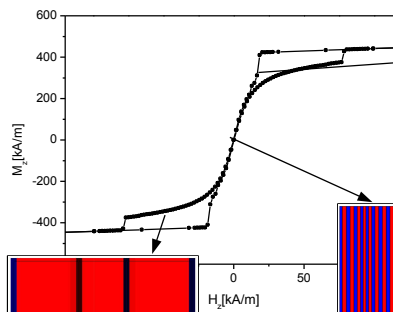


[Co(1nm)/spacer(1nm)/NiFe(1nm)/spacer(1nm)]₄/Co(1nm)

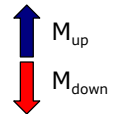
No attempts were made to exactly mirror the M(H) dependence, i.e., nucleation and annihilation fields.

Magnetostatic coupling

Micromagnetic simulation

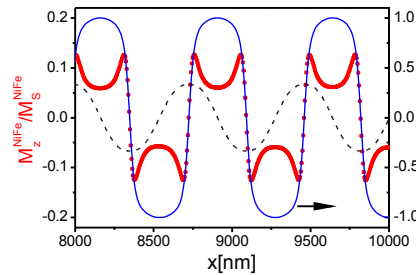


Stripe domains

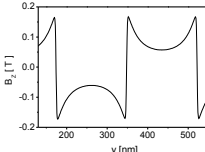


Magnetostatic coupling

Micromagnetic simulation



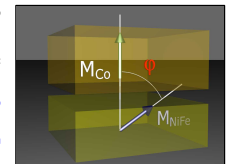
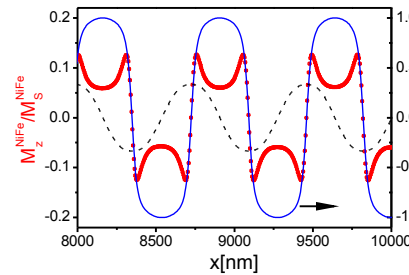
Field calculated from Biot-Savart law for zero DW width



Magnetostatic interactions between Co and NiFe layers lead to the spatial replication of the z-component of magnetic moment of Co sublayers in NiFe sublayers \Rightarrow resistance decrease.

Magnetostatic coupling

Micromagnetic simulation

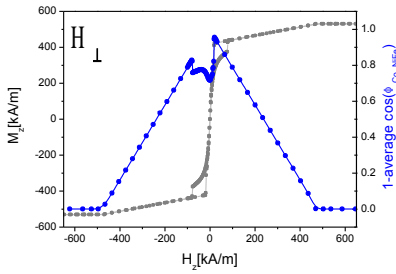


$$\Delta R_{GMR} = \frac{1}{n} \sum \cos(\phi_{NiFe-Co})$$

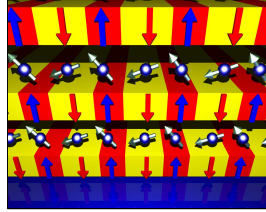


Magnetostatic coupling

Micromagnetic simulation



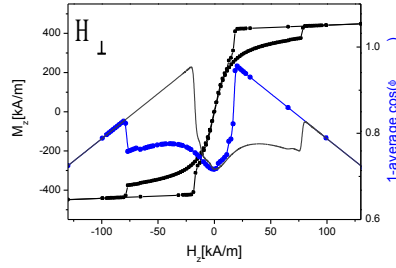
The GMR(H) dependence was calculated as proportional to an average cosine of the angle between magnetic moment direction of juxtaposed NiFe and Co cells.



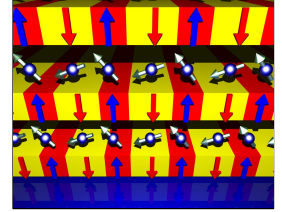
Giant magnetoresistance dependencies of NiFe/Au/Co/Au multilayers can be approximated from micromagnetic simulations.

Magnetostatic coupling

Micromagnetic simulation



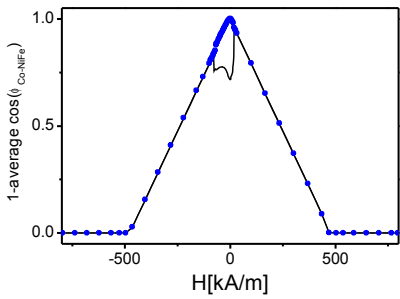
The GMR(H) dependence was calculated as proportional to an average cosine of the angle between magnetic moment direction of juxtaposed NiFe and Co cells.



Giant magnetoresistance dependencies of NiFe/Au/Co/Au multilayers can be approximated from micromagnetic simulations.

Magnetostatic coupling

Micromagnetic simulation

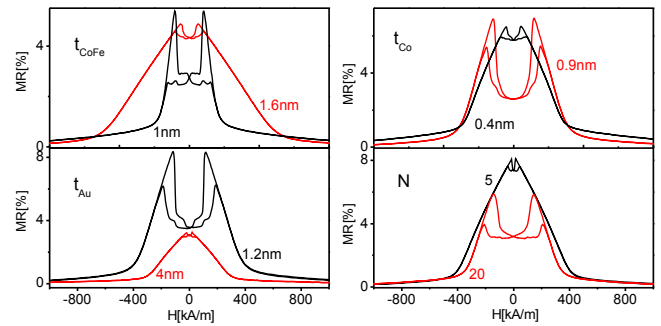


The GMR(H) dependence was calculated as proportional to an average cosine of the angle between magnetic moment direction of juxtaposed NiFe and Co cells.

..... - no coupling

Without magnetostatic coupling between Co and NiFe layers there are no local minima of resistance.

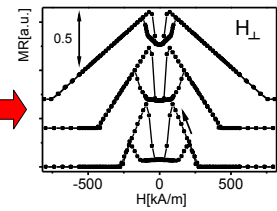
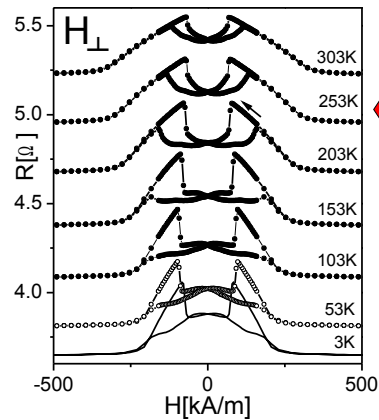
Magnetostatic coupling



The strength of coupling between sublayers with perpendicular and in-plane anisotropy (depth of resistance minimum) depends on thicknesses of all types of sublayers and on the number of repetitions.

Magnetostatic coupling

Micromagnetic simulation

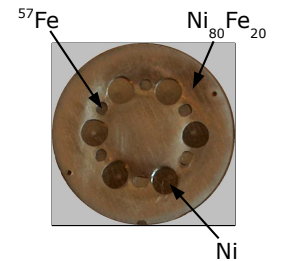
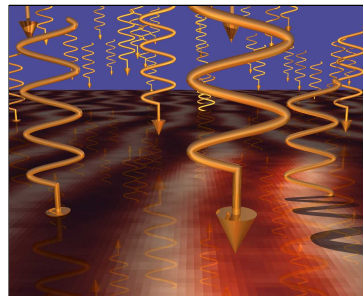


OOMMF simulation with changing perpendicular anisotropy of CoFe sublayers. from top to bottom: $K_u=0.7 \times 10^6 \text{ J/m}^3$, $K_u=1 \times 10^6 \text{ J/m}^3$ and $K_u=1.15 \times 10^6 \text{ J/m}^3$.

[Co₈₃Fe₁₇(1.2 nm)/Au(2.2 nm)/Co(0.8 nm)/Au(2.2 nm)]₁₀

Element selective measurements

Mössbauer spectroscopy



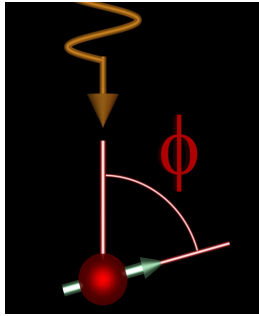
Conversion electron Mössbauer spectroscopy (CEMS)
⁵⁷Co source
⁵⁷Fe 95.3 at.%



[Ni₈₀Fe₂₀/Au/Co/Au]₁₀

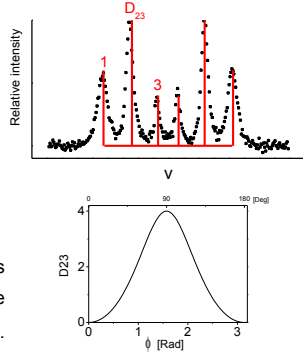
Element selective measurements

Mössbauer spectroscopy



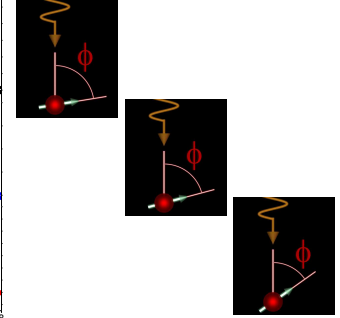
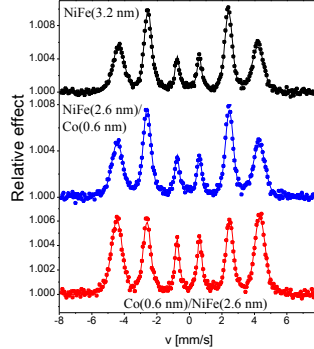
Relative intensities of the hyperfine lines vary with the angle ϕ between the incident γ -ray and the magnetic moment.

$$D_{23} = \frac{4 \sin^2(\phi)}{1 + \cos^2(\phi)}$$



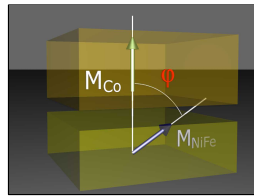
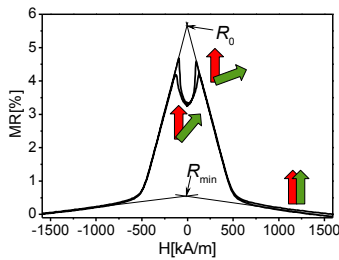
Element selective measurements

Mössbauer spectroscopy



$[\text{Ni}_{80}\text{Fe}_{20}(3.2 \text{ nm})/\text{Au}(2.4 \text{ nm})/\text{Co}(0.8 \text{ nm})/\text{Au}(2.4 \text{ nm})]_{10}$
 $[\text{Ni}_{80}\text{Fe}_{20}(2.6 \text{ nm})/\text{Co}(0.6 \text{ nm})/\text{Au}(2.4 \text{ nm})/\text{Co}(0.8 \text{ nm})/\text{Au}(2.4 \text{ nm})]_{10}$
 $[\text{Co}(0.6 \text{ nm})/\text{Ni}_{80}\text{Fe}_{20}(2.6 \text{ nm})/\text{Au}(2.4 \text{ nm})/\text{Co}(0.8 \text{ nm})/\text{Au}(2.4 \text{ nm})]_{10}$

Element selective measurements



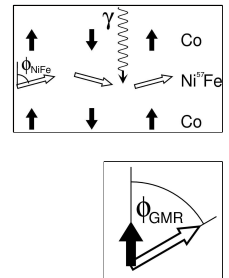
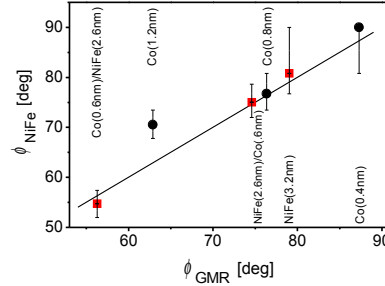
$$R = R_0 - (R_0 - R_{min}) \cos(\phi_{\text{Co-NiFe}})$$

Resistance measurements allow the determination of the average cosine of the angle between magnetic moments of **Co** and **NiFe** layers.

$[\text{Ni}_{80}\text{Fe}_{20}(2 \text{ nm})/\text{Au}(2.4 \text{ nm})/\text{Co}(1.2 \text{ nm})/\text{Au}(2.4 \text{ nm})]_{10}$

Element selective measurements

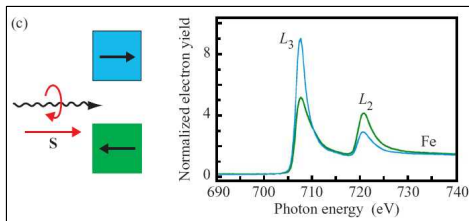
Mössbauer spectroscopy vs. GMR



The magnetostatic fields of the Co domains cause the deflection of the magnetic moments of the NiFe layers. The deflection is stronger if the effective easy-plane anisotropy of NiFe layers is weaker.

$[\text{X}/\text{Au}(2.4 \text{ nm})/\text{Co}(0.8 \text{ nm})/\text{Au}(2.4 \text{ nm})]_{10}$
 $[\text{Ni}_{80}\text{Fe}_{20}(2 \text{ nm})/\text{Au}(2.4 \text{ nm})/\text{Co}/\text{Au}(2.4 \text{ nm})]_{10}$

Soft x-ray resonant magnetic scattering (SXRMS)



Circularly polarized light
 $\lambda \approx 1.4 \text{ nm}$
 interaction with core electrons
 photon energy tuned to absorption edge
elemental selectivity

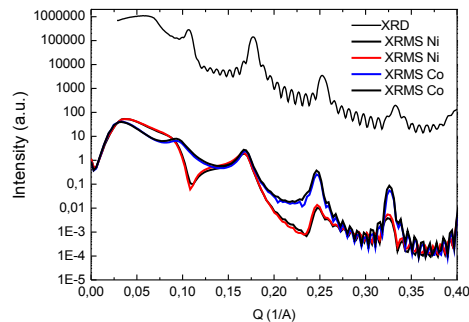
* SXRMS at BESSY - measurement of the intensity of a reflected X-ray versus the external magnetic field (θ - 2θ geometry).

Sampling depth $\sim 10 \text{ nm}$

ALICE diffractometer at the undulator beamline UE56/2-PGM2 at BESSY II (Berlin)

*graphics source: ssrl.slac.stanford.edu/stohr/xmed.htm see ssrl.slac.stanford.edu/stohr/X-Rays_and_Magnetism.ppt

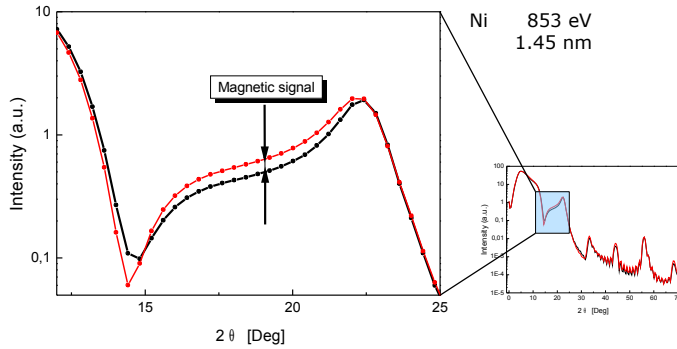
Soft x-ray resonant magnetic scattering (SXRMS)



Cu K α 8048 eV
 Ni 853 eV
 Co 778 eV

$[\text{Ni}_{80}\text{Fe}_{20}(2 \text{ nm})/\text{Au}(2 \text{ nm})/\text{Co}(0.8 \text{ nm})/\text{Au}(2 \text{ nm})]_{10}$

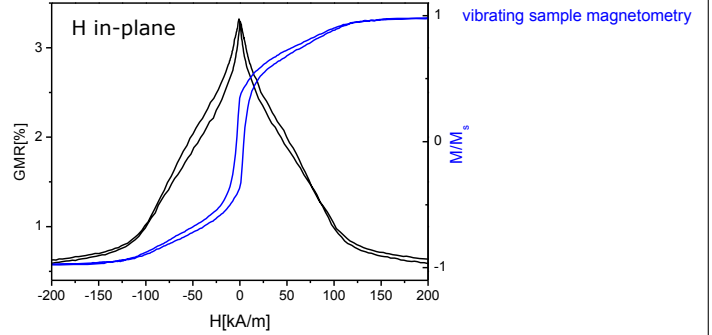
Soft x-ray resonant magnetic scattering (SXRMS)



$[\text{Ni}_{80}\text{Fe}_{20}(2 \text{ nm})/\text{Au}(2 \text{ nm})/\text{Co}(0.8 \text{ nm})/\text{Au}(2 \text{ nm})]_{10}$

ALICE diffractometer at the undulator beamline UE56/2-PGM2 at BESSY II (Berlin)

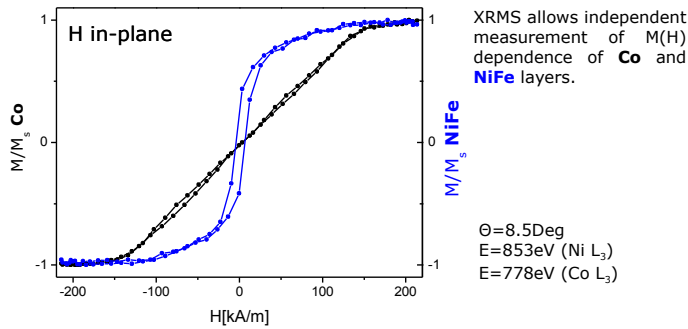
Soft x-ray resonant magnetic scattering (SXRMS)



$R(H) \leftrightarrow M(H)$

$[\text{Ni}_{80}\text{Fe}_{20}(2 \text{ nm})/\text{Au}(2 \text{ nm})/\text{Co}(1.1 \text{ nm})/\text{Au}(2 \text{ nm})]_{10}$

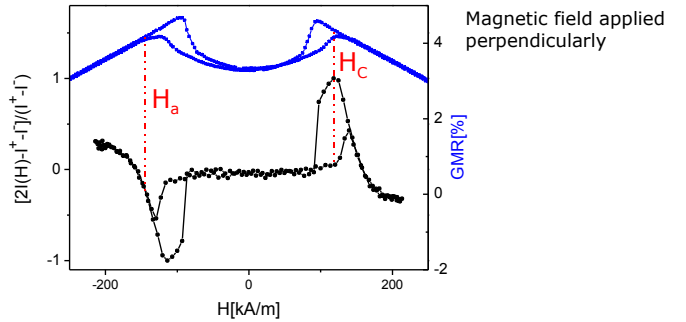
Soft x-ray resonant magnetic scattering (SXRMS)



$$M/M_s \propto [2I(H) - I^+ - I^-] / (I^+ - I^-)$$

$[\text{Ni}_{80}\text{Fe}_{20}(2 \text{ nm})/\text{Au}(2 \text{ nm})/\text{Co}(1.1 \text{ nm})/\text{Au}(2 \text{ nm})]_{10}$

Soft x-ray resonant magnetic scattering (SXRMS)

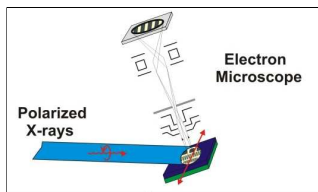


SXRMS signal from **NiFe layers** shows fields characteristic for Co layers reversal:
 - creation of the stripe domain structure (H_c)
 - annihilation field of domain structure (H_a)

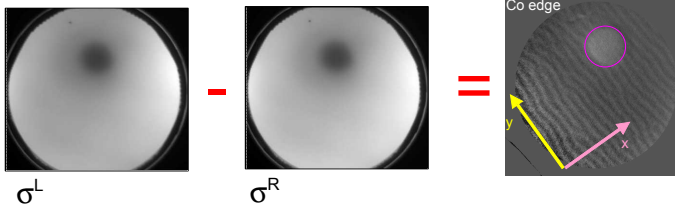
$[\text{Ni}_{80}\text{Fe}_{20}(2 \text{ nm})/\text{Au}(2 \text{ nm})/\text{Co}(1.1 \text{ nm})/\text{Au}(2 \text{ nm})]_{10}$

XMCD-PEEM

Sincrotrone Trieste ELETTRA S.C.p.A. di interesse nazionale

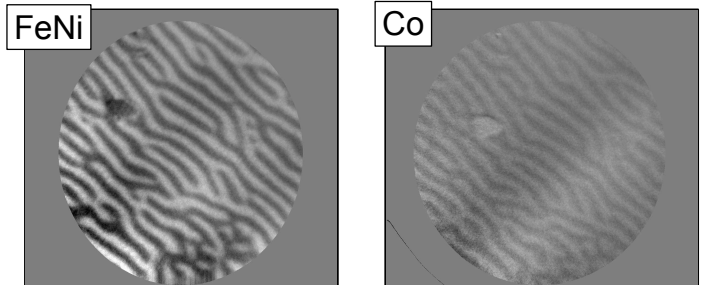


*graphics from: ssrl.slac.stanford.edu/stohr/xmcd.htm



XMCD-PEEM

Sincrotrone Trieste ELETTRA S.C.p.A. di interesse nazionale

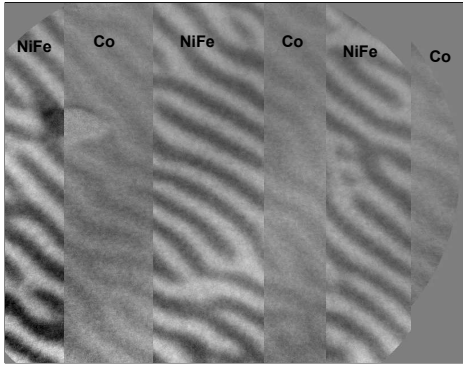


Experimental confirmation of the replication of the Co stripe domains in the perpendicular component of NiFe sublayers magnetization.

$[\text{Ni}_{80}\text{Fe}_{20}(2 \text{ nm})/\text{Au}(2 \text{ nm})/\text{Co}(0.8 \text{ nm})/\text{Au}(2 \text{ nm})]_{10}/\text{Ni}_{80}\text{Fe}_{20}(2 \text{ nm})$
 after in-plane ex-situ magnetizing in 0.7T

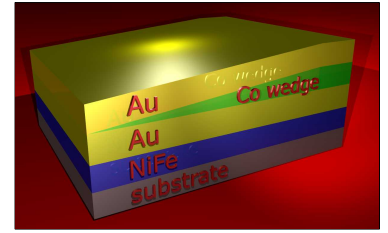
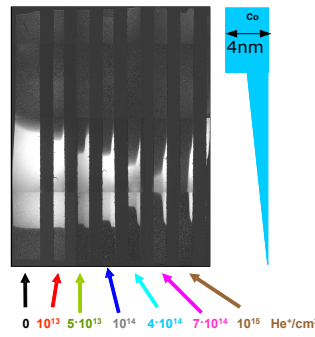
XMCD-PEEM

Sincrotrone Trieste **ELETTRA**
S.C.p.A. di interesse nazionale



Experimental confirmation of the replication of the Co stripe domains in the perpendicular component of NiFe sublayers magnetization.

He Ion bombardment*

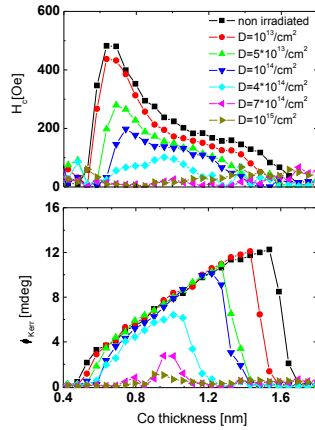
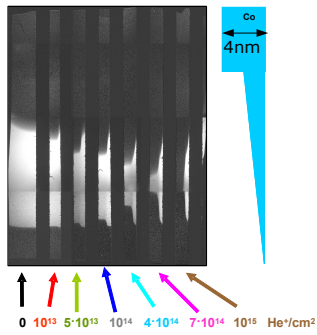


Magneto-optical Kerr effect observation of magnetic structuration caused by ion bombardment:
10keV He⁺
non-topological patterning

Si(100)/buffer/Ni₈₀Fe₂₀-2nm/Au-3nm/Co wedge/Au-3nm

*P. Kuświk et al., ACTA PHYSICA POLONICA A 113, 651 (2008)

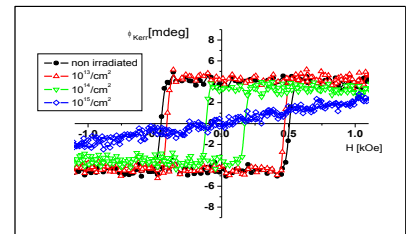
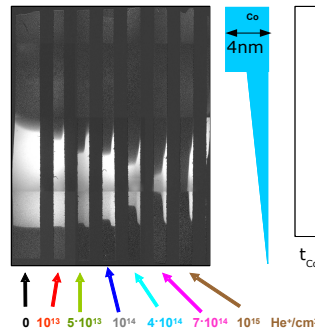
He Ion bombardment*



Si(100)/buffer/Ni₈₀Fe₂₀-2nm/Au-3nm/Co wedge/Au-3nm

*P. Kuświk et al., ACTA PHYSICA POLONICA A 113, 651 (2008)

He Ion bombardment*



$t_{Co} = 0.6nm$, $M(H)$ for Co sublayers only

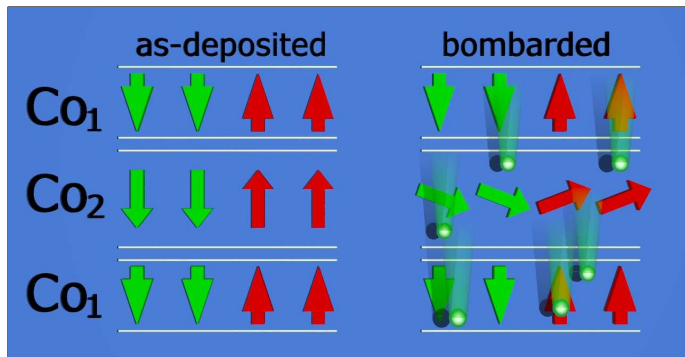
Negligible changes of magnetic properties for doses $\leq 10^{13}$ ion/cm²

Si(100)/buffer/Ni₈₀Fe₂₀-2nm/Au-3nm/Co wedge/Au-3nm

*P. Kuświk et al., ACTA PHYSICA POLONICA A 113, 651 (2008)

He Ion bombardment*

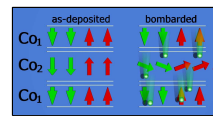
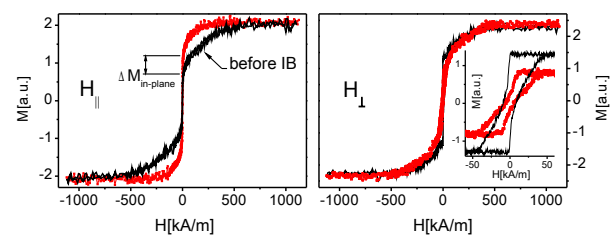
He⁺ (10 keV, 6×10^{14} ions cm⁻²)



[Co1(0.6 nm)/Au(4 nm)/Co2(1 nm)/Au(4 nm)]₄

*together with Ehresmann AG, Kassel (www.physik.uni-kassel.de/ehresmann)

He Ion bombardment*

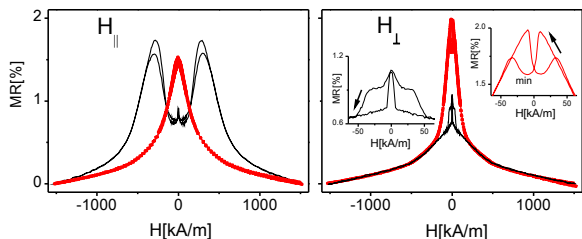


$$K_{eff} = \frac{2K_{1s}}{t_{Co}} + K_{1v} - \frac{1}{2}\mu_0(M_S^{Co})^2$$

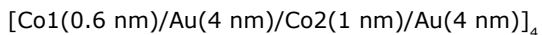
[Co1(0.6 nm)/Au(4 nm)/Co2(1 nm)/Au(4 nm)]₄

*together with Ehresmann AG, Kassel (www.physik.uni-kassel.de/ehresmann)

He Ion bombardment

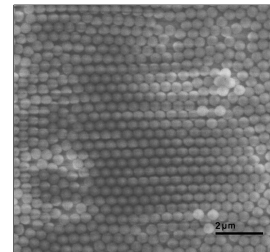
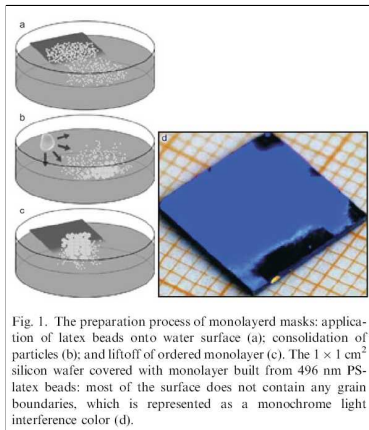


The resistance measurements confirm the observation inferred from the M(H) measurements: the IB led to the switching of the EA direction in the 1 nm thick Co layers while the 0.6 nm thick layers preserved the perpendicular effective anisotropy.



He Ion bombardment

Magnetic patterning



*W. Glapka, P. Kuświk *et al.*, ACTA PHYSICA POLONICA A 115, 348 (2009)

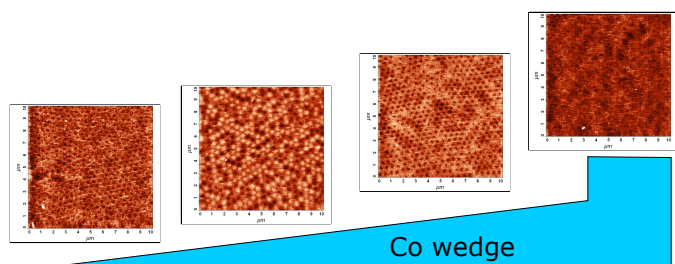
polystyrene nanospheres (diameter 470 nm) were deposited on the multilayer surfaces via a self-assembly process realized by a dip coating.

Fig. 1. The preparation process of monolayer masks: application of latex beads onto water surface (a); consolidation of particles (b); and liftoff of ordered monolayer (c). The $1 \times 1 \text{ cm}^2$ silicon wafer covered with monolayer built from 496 nm PS-latex beads: most of the surface does not contain any grain boundaries, which is represented as a monochrome light interference color (d).

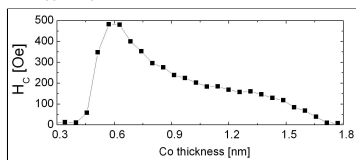
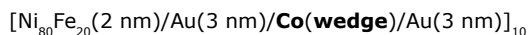
J. Rybczyński *et al.* Colloids and Surfaces A: Physicochem. Eng. Aspects 219, 1 (2003)

He Ion bombardment

Magnetic patterning



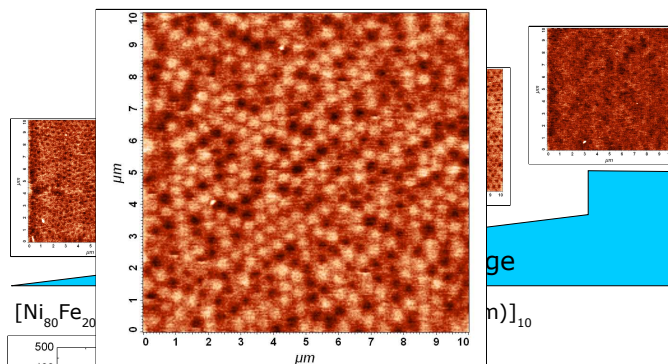
Co wedge



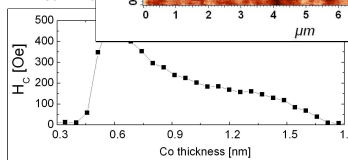
*W. Glapka, P. Kuświk *et al.*, ACTA PHYSICA POLONICA A 115, 348 (2009)

He Ion bombardment

Magnetic patterning



Co wedge



*W. Glapka, P. Kuświk *et al.*, ACTA PHYSICA POLONICA A 115, 348 (2009)

Conclusions

- $F_{||}/\text{Au}/F_{\perp}/\text{Au}$ MIs represent new type of spin-valves
- Magnetostatic coupling influences magnetic reversal of $F_{||}/\text{Au}/F_{\perp}$ MIs
- $F_{||}/\text{Au}/F_{\perp}$ MIs are suitable for a non-topological magnetic patterning

Zakopane
2009

Magnetic properties of $[\text{NiFe}/\text{Au}/\text{Co}/\text{Au}]$ Multilayers - magnetostatic coupling and giant magnetoresistance

Thank you for your attention